Penrose tiling approximants

O. Entin-Wohlman, M. Kléman, A. Pavlovitch

J. Phys. France **49** (1988) 587-598 AVRIL **1988**, PAGE 587

Classification
Physics Abstracts
61.16 — 61.50E — 61.70E

Penrose tiling approximants

O. Entin-Wohlman (*), M. Kléman and A. Pavlovitch (1)

Laboratoire de Physique des Solides, associé au CNRS, Université de Paris-Sud, 91405 Orsay, France
(1) D. Tech/SRMP-CEN Saclay, BP 2, 91191 Gif-sur-Yvette Cedex, France

(*Reçu le 22 juin 1987, accepté sous forme définitive le 17 novembre 1987*)

Résumé. — Nous considérons les structures obtenues en modifiant un pavage de Penrose en un pavage périodique. Les analyses détaillées de la méthode de la bande et de la transformation duale sont présentées de façon à produire une classification générale des approximants. La nature des défauts qu'il est nécessaire d'introduire pour transformer un cristal apériodique en un cristal périodique est discutée ; nous calculons en outre leur nombre par cellule unité ainsi que la densité des tuiles. Notre modèle implique que les dislocations partielles des approximants et les dislocations élémentaires des quasi-cristaux sont des objets fondamentalement similaires ; cette similarité devrait conduire à des propriétés de déformation plastique comparables.

Abstract. — The modification of the Penrose tiling into a periodic structure is considered. Detailed analysis of the strip method and the dual transformation which yield approximants of the perfect tiling is presented in such a way that a complete classification of approximants is provided. The defects introduced to change the aperiodic order into a periodic one are discussed, their number per unit cell is derived, and the tile density is calculated. Our model implies also a fundamental similarity between the partial dislocations of the approximants and the elementary dislocations of quasi-crystals, which might result in comparable plasticity properties.

1. Introduction.

This paper intends to describe in details the geometry of the Penrose tiling (rational) approximants, and how they are related to perfect Penrose tilings *via* some defects which are described. It provides also a classification of these approximants in function of the size of their unit cell and the number of defects per unit cell. It shows also that there is a simple relationship between the periodicities of the approximants and some characteristic lattice vectors of the Penrose tiling ; this relationship might introduce some new ideas concerning the plasticity behaviour of the approximants. For simplicity, the whole analysis is restricted to 2-d tilings, but most of the methods and ideas extend readily to 3-d.

1) Let us first comment on why we think that a detailed knowledge of the geometry of the rational approximants is of importance for physical systems. Practically all known *i*-phases possess crystalline modifications with a large unit-cell and close chemical composition and local order ; they often coexist coherently with the *i*-phase ; let us quote *i*-(Al, Zn)$_{49}$Mg$_{32}$, whose related crystalline phase is a Laves phase with a large unit cell [1], Cu$_4$Cd$_3$, which in its crystalline phase possesses 1 124 atoms per cell and 568 icosahedral units [2], Al-Mn-Si [3, 4], Al$_{13}$Fe$_4$ [4], Al-Li-(Cu, Mg) [5], Ga-Mg-Zn [6], etc... In [4] a decoration of the Penrose tiles with Al and Fe is presented. The structure thus obtained is a Penrose tiling with defects. It is interesting to notice that many of the crystalline modifications so far described are topologically close-packed structures which enter the category of Frank and Kasper phases [7]. Therefore the study of these crystalline modifications and how they relate to approximants should also shed some light on the Frank and Kasper phases, and in return benefit to the understanding of quasi-crystals ; see for example Henley [4].

2) A concept which has proved useful in the description of the systematic disorder experimentally observed in aperiodic crystals [8], is the one of « phason strains » (continuous version) or « phasons » (discrete version). The same « phasons » [9] are the defects we alluded to, which, when introduced in a regular way in icosahedral or Penrose lattices, change them into periodic « approximants ». Although this idea is not new [4, 10, 11] it has not been pushed yet towards a structural description of approximants, i.e., to describe in detail the relationship between crystalline related phases and aperiodic phases. Biham *et al.* [11] have studied the stability of Penrose lattices *versus* periodic, approximant, lattices using continuous phase gradients in the Landau formalism. Phonons (i.e., elastic distortions) can be indeed naturally described by a continuous theory but « phasons » are more delicate [12]. They are specific defects of the perfect tiling which, in the cut and strip picture of the aperiodic crystals, occur by introducing a vertex in and remov-

(*) *Permanent address :* School of Physics and Astronomy, Tel Aviv University, Tel Aviv 69978, Israel.

ing another from the strip. This paper is directed towards a systematic study of the production rules, classification and defect content (with respect to a perfect aperiodic tiling) of the approximants. We also believe that our results are relevant to the general question concerning the role of defects in incommensurate-commensurate transition [13].

We explain in the next section the concept of Fibonacci approximants in conjunction with defects by considering an one-dimensional example — the approximants to the Fibonacci sequence. In the third section, we explore in detail the approximants of the Penrose tiling. In particular, we derive in a systematic way the Fibonacci approximants of the Penrose tiling, and calculate the number of defects per unit cell required to change the aperiodic structure into a periodic one. We discuss how some characteristic vectors of the perfect tiling (i.e. the long diagonals of the thin rhombuses and the short diagonals of the thick rhombuses in the Penrose-de Bruijn picture of the tiling [17]) are related to the lattice spacing of the approximant, and calculate the tile density of the Fibonacci approximants. We discuss the nature of the defects involved in the incommensurate-commensurate transformation and study the specific character of the inflation properties of the approximants.

In the course of the text, we shall give demonstrations as complete as possible ; some of them can be escaped by the reader in hurry, who will find a detailed summary of our results in section 4.

2. Approximants of the Fibonacci sequence.

One of the methods to construct structures with 5-fold symmetry is by projecting them from a higher-dimensionality periodic structure. One gets 2-d structures from a 4-d space and 3-d structures by projection from a 6-d space. The 1-d aperiodic analogous structure is the Fibonacci sequence, obtained by projection from a 2-d periodic structure [4, 14]. The Fibonacci sequence consists of a series of long (L) and short (S) intervals. The relative concentration of S to L intervals is equal to $G = \tau^{-1}$, where $\tau = (\sqrt{5} + 1)/2$ is the golden ratio. The aperiodic 1-d ordering may be obtaining [4, 14] by projecting from a two-dimensional periodic lattice onto a straight line of slope τ, the « physical » line, those lattice points whose projections on the axis perpendicular to the physical line fall within a specified window. Thus, one defines an irrational « strip » which includes the lattice points whose projections on the physical line yields the Fibonacci sequence. To obtain a periodic one-dimensional sequence which is an approximant of the Fibonacci series, one replaces the irrational strip by a rational one (i.e., whose slope with respect to the axes of two dimensional space is rational). We then can choose the physical line (onto which the lattice points within the rational strip are projected) to have the same slope as in the irrational case. This choice has by no means any compulsory character, but has the advantage that the tiling shapes of the approximant are the same L and S segments as for the irrational strip.

Any rational approximant defined in this way consists of periodically repeated « irrational » blocks. However, the natural choice for the slope of the rational strip is the ratio f_{n+1}/f_n of two Fibonacci numbers [15]. Figure 1a illustrates the division into blocks of a Fibonacci approximant. The rational line, of slope f_{n+1}/f_n, is the best approximation of the irrational line of slope τ in the sense that there are no vertices of the 2-d lattice inside the triangle $OA\alpha$, where O is the common origin to the

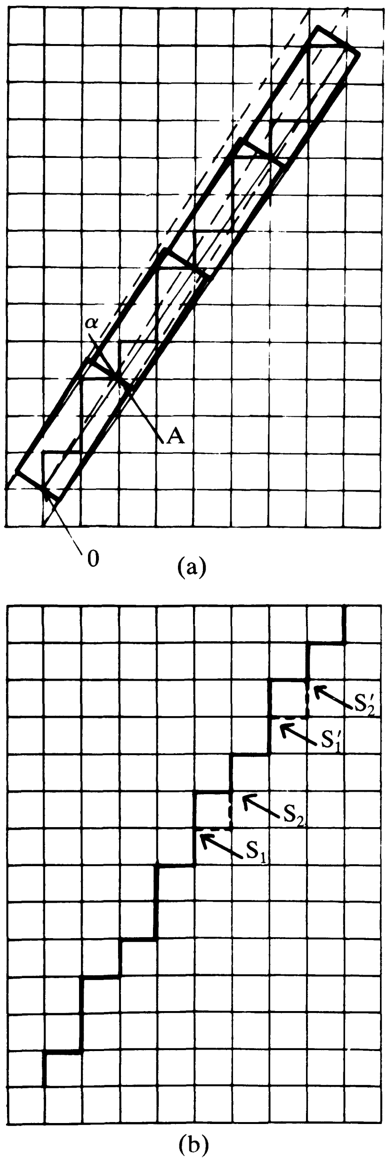

Fig. 1. — a) Division of a Fibonacci approximant into irrational blocks. Dashed line-approximant strip ; full line-Fibonacci strip. b) The full line is the Fibonacci sequence. The dashed lines show the flips required to obtain the approximant of figure 1a. The arrows indicate the division of a flip into two staking faults.

two lines, A the limit of the blocks, and α the projection of A on the irrational line.

The unit cell of the approximant has $f_n + f_{n+1} = f_{n+2}$ intervals, including f_n S-segments and f_{n+1} L-segments. The size of the unit cell thus increases with the order n of the Fibonacci numbers, and approaches infinity as the ratio f_{n+1}/f_n becomes closer and closer to τ.

Clearly, the sequence of L and S intervals of the approximant, being periodic, is different from that of the aperiodic structure. Starting from the origin, then until a certain point, the approximant sequence coincides with that of the aperiodic structure. Then a « flip » takes place. For example, SL of the aperiodic sequence changes into LS in the approximant sequence. Then, in the approximant sequence, the structure repeats itself. We can view this as moving this irrational Fibonacci block of the irrational strip in the two-dimensional space, so that it will cover the periods of the rational strip. The transformation which brings one Fibonacci block to the next consists of a translation along the physical line, i.e., a « phonon » part [9] and a perpendicular translation, i.e., a « phason » part. It is of course the « phason » part which is effective to regain periodicity. The similarity between the situation we are describing and a one-dimensional incommensurate-commensurate transition with « epitaxy » dislocations is striking [13] ; however, the two sublattices which are matched by epitaxy in the usual description [16] are here the same lattice and, in last sense, the incommensurability is not a simple perturbation of a periodic lattice. It is therefore worth having a clear definition of the defect we have introduced by the flip. It is in fact akin to a double stacking fault, or a wall, since it can be considered as the defect which occurs at the intersection of the physical, irrational, line with a perpendicular line. We shall see that a similar description holds in the two-dimensional case. As a double stacking fault, this defect can be divided into two elementary stacking faults (Fig. 1b) which would propagate independently. Note that we have introduced only one flip in each period ; this is because of the particular choice f_{n+1}/f_n of the slope of the rational strip. A choice of a non-Fibonacci approximant would have required more flips per period.

Let us call an n-approximant a periodic line with f_n segments per period ; such a period is a Fibonacci subsequence with one flip. A remarkable fact about two successive approximants n and $n+1$ is that $n+1$ is the deflation of n and is obtained from n by the rule $\mathrm{L} \to \mathrm{LS}$, $\mathrm{S} \to \mathrm{L}$, which is true everywhere, except on the stacking faults. More will be said about inflation in the two-dimensional case.

Note that any finite sequence of L's and S's on the Fibonacci infinite sequence, of length f_n, can be chosen as the starting sequence of a Fibonacci approximant ; it is enough to introduce one flip anywhere on this sequence to get the period of a Fibonacci approximant. The operation which consists in moving the rational strip along a direction orthogonal to itself is the operation which transforms any periodic sequence of L's and S's into another one. In terms of phase and phonon modes, it can be described as a global phase change ; we shall find the same types of structural properties in the description of commensurate two-dimensional lattices (rational approximants) of Penrose tilings.

3. Penrose tiling approximants.

3.1 THE PERFECT TILING. — The detailed geometrical description of the Penrose tiling was given by de Bruijn [17]. The tiling consists of two rhombic shapes (Fig. 2), and its vertices can be obtained either as duals to the meshes of a regular pentagrid, or by projection from a 5-dimensional simple-cubic lattice ; we shortly describe the two methods.

i) Any Penrose tiling is the dual of a pentagrid. The regular pentagrid consists of five sets F_i of parallel equidistant lines, perpendicular to the five directions $\boldsymbol{\nu}_i$ $(i = 0, \dots, 4)$ of a regular pentagon, $\boldsymbol{\nu}_i = (\cos \frac{2\pi i}{5}, \sin \frac{2\pi i}{5})$. In each of the sets F_i, the parallel lines are labelled by successive integer numbers k_i, with respect to a certain origin. Thus, to each mesh of the pentagrid corresponds a quintople of 5 integers k_i, which label the F_i-lines closest to the interior of the mesh (in each $\boldsymbol{\nu}_i$-direction, the higher-k_i line is chosen). The Penrose tiling vertex dual to the grid mesh is then given by $\mathbf{r} = \sum_i k_i \boldsymbol{\nu}_i$.

ii) The Penrose tiling may be equivalently obtained by projecting from a periodic 5-dimensional

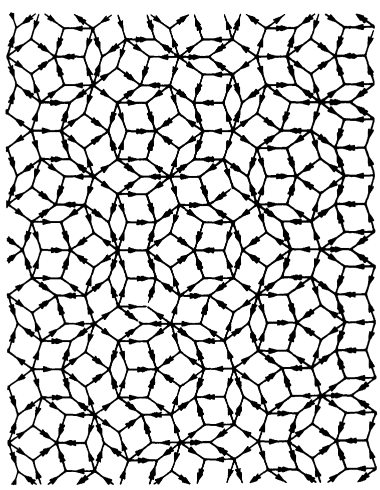

Fig. 2. — Perfect Penrose tiling.

structure onto an irrational physical plane P, given by the vectors [17] :

$$\mathbf{u}_1 = \sum_j \sqrt{\frac{2}{5}} \cos \frac{2\,\pi j}{5}\, \mathbf{e}_j , \qquad j = 0, 1, 2, 3, 4 .$$
$$\mathbf{u}_2 = \sum_j \sqrt{\frac{2}{5}} \sin \frac{2\,\pi j}{5}\, \mathbf{e}_j , \tag{1}$$

where $\mathbf{e}_j = (\delta_{0j}, \delta_{1j}, \delta_{2j}, \delta_{3j}, \delta_{4j})$ are the vectors of the 5-d canonical base and j denotes the vector components.

The 5-dimensional (simple cubic) lattice points which are projected are those belonging to a « strip » defined by a cut in a plane P′ perpendicular to P and to the (1, 1, 1, 1, 1) direction.

iii) Penrose tilings possess a number of structural features which will be used in this paper. These are

— infinite sequences of adjacent rhombuses with a common edge direction parallel to $\boldsymbol{v}_i$. Such sequences have a constant width and their rhombuses are dual of all the intersections of the pentagrid located along a line belonging to the set F_i of the pentagrid ;

— hexagons D and Q (Fig. 3) made of three rhombuses. They bear their names from the fact that their central vertex is either a D-vertex (a deuce in de Bruijn nomenclature) or a Q-vertex (a queen) ;

— « worms » : these are, in the language of Socolar *et al.* [9], finite or infinite sequences of hexagons of both types. Their interest lies in the fact that they are paths of propagation for the shifts of hexagons which will be described in the next subsection. The geometry of the worms and their statistics have been studied in [18] ;

— « decagons » : the decagons are non-centrosymmetric assemblies of 10 rhombuses which bind the finite worms (Figs. 3 and 4).

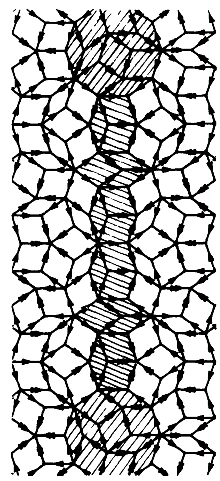

Fig. 4. — Worm bounded by two decagons.

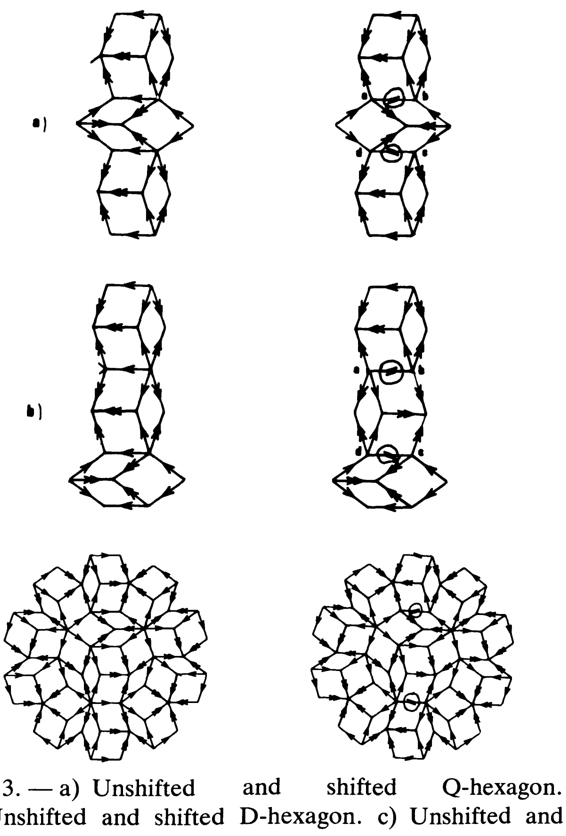

Fig. 3. — a) Unshifted and shifted Q-hexagon. b) Unshifted and shifted D-hexagon. c) Unshifted and shifted decagons.

3.2 DEFECTS IN APPROXIMANTS : SHIFTS AND MISMATCHES. — The generalization of a flip in the Fibonacci sequence to the two-dimensional Penrose tiling, is either a shift of the central vertex D or Q of an hexagon made of three rhombuses, or a rotation of a decagon. These types of structures include vertices that are the projections of 5-dimensional lattice points which are closest to the boundaries of the irrational strip [17]. This is why these shifts appear first when the irrational strip is moved by a small amount : if a vertex disappears on one side of the strip, another one enters the strip on the other side and projects as a shifted vertex in the Penrose tiling. In fact, any displacement of the strip, whatever large it might be, can be decomposed into such D and Q shifts, and decagon rotations. We shall construct approximants to the Penrose tiling by considering, as in the one-dimensional case, strips of rational slopes. The vertices belonging to that strip are projected on the irrational plane P, which is therefore tiled with the same thick (T) and thin (t) rhombuses as in the Penrose tiling. The commensurability will appear through the presence of shifts ; we shall see that the minimal number of shifts in a rational approximant is one per unit cell (Fig. 5).

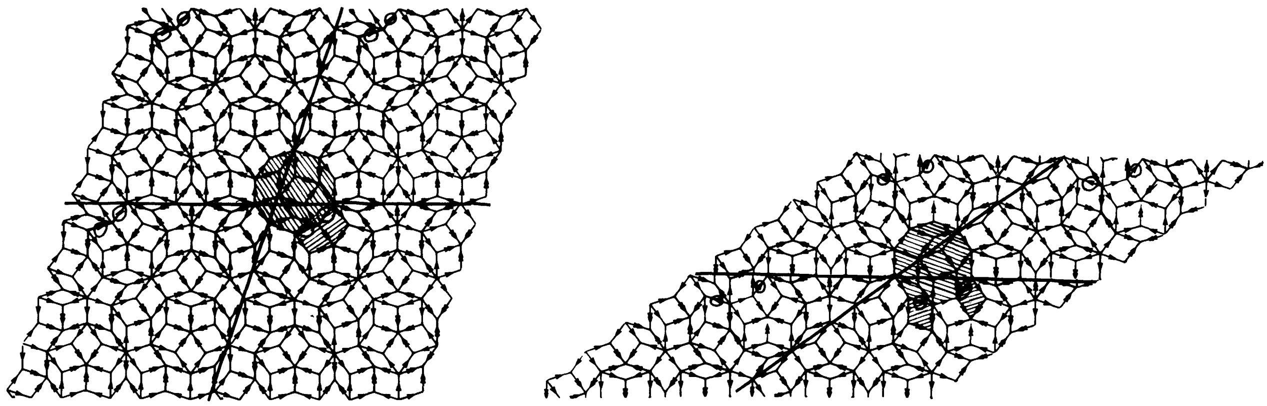

Fig. 5. — Approximant tiling with two mismatches located in the same decagon. a) Unit cell of the shape of a thick rhombus ; b) Unit cell of the shape of a thin rhombus.

But note immediately that each shift introduces two « mismatches » of the de Bruijn arrowing pattern along the « worm » to which it belongs. A shift can « extend » along a worm, by a process which is probably diffusive in a real crystal. In such a case, the two parallel « mismatches » separate and go apart at some distance along the worm (Fig. 6). Complex processes happen when a mismatch hits the end of a worm [9]. In general, in such a case, several new shifts happen in the decagon which closes the worm, and propagate outside along several new directions. In any case, as long as the distances of separation and the rearrangements do not exceed the unit cell of the approximant, this process defines a new unit cell of same size and shape as the initial one. Rational approximants, whose shifts are not extended, are built from strips whose boundaries are lattice planes of the hypercubic lattice. (In such a case, the projected vertices include the vertices either of the upper, or of the lower boundary, but not both.) Rational approximants with extended shifts originate from generic rational strips (i.e., whose boundaries are parallel to lattice planes, but not passing through lattice points).

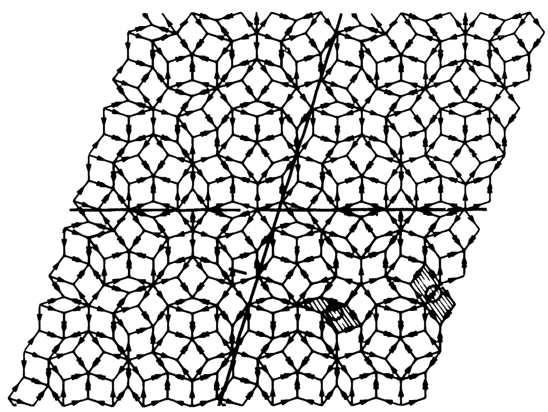

Fig. 6. — Same as figure 5a, with separated mismatches.

3.3 GEOMETRY OF A RATIONAL APPROXIMANT. — Consider a plane P_{pq} (for simplicity, we assume it to be a lattice plane) defined by two vectors $\mathbf{p}$, $\mathbf{q}$:

$$\begin{aligned} \mathbf{p} &= (p_0, p_1, p_2, p_3, p_4)\,, \\ \mathbf{q} &= (q_0, q_1, q_2, q_3, q_4)\,. \end{aligned} \tag{2}$$

In order to keep 5-fold orientational correlations, we impose that P_{pq} is orthogonal to the $(1, 1, 1, 1, 1)$ direction, i.e.,

$$\begin{aligned} \sum p_i &= 0\,, \\ \sum q_i &= 0\,. \end{aligned} \tag{3}$$

The intersections of the 4-dimensional hyperplanar facets of the 5-dimensional hypercubic lattice with the P_{pq} plane are along the five directions $\boldsymbol{\omega}_i$

$$\boldsymbol{\omega}_i = q_i\,\mathbf{p} - p_i\,\mathbf{q}\,. \tag{4}$$

This is easily seen by noting that $\boldsymbol{\omega}_i \cdot \mathbf{e}_j = q_i\,p_j - q_j\,p_i$, where $\mathbf{e}_j = (\delta_{0j}, \delta_{1j}, \delta_{2j}, \delta_{3j}, \delta_{4j})$ are the standard unit vectors of the 5-dimensional space and hence $\boldsymbol{\omega}_i \cdot \mathbf{e}_i = 0$.

We now follow de Bruijn [17] and construct the pentagrid in the P_{pq}-plane, whose dual will yield the approximant tiling. It consists of five sets F_i ($i = 0, 1, 2, 3, 4$) of lines parallel to the $\boldsymbol{\omega}_i$'s. It is not difficult to show that the intersections of the F_i lines with the axis $\mathbf{p}$ have abscissae $k_i \dfrac{\mathbf{p}}{p_i}$ where k_i is an integer. Obviously, k_i is the only non zero coordinate of the 4-dimensional hyperplane perpendicular to $\mathbf{e}_i$, whose intersection with P_{pq} is the line in question (assuming that the origin of the 5-dimensional space and the origin in the P_{pq} plane coincide), since $k_i \dfrac{\mathbf{p}}{p_i} \cdot \mathbf{e}_i = k_i$. We have drawn in figure 7 such a set of lines limited to their segments inside one of the unit cell of the P_{pq} plane. For rational values of p_i and q_i, the lattice is periodic and the unit cell has the topology of a torus T_2. It is thus seen that the segments of the lines form a closed path on this

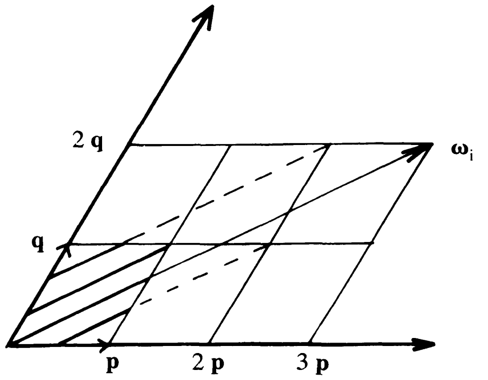

Fig. 7. — The p and q lines on the torus T_2.

torus, along an oriented line L of the homotopy class (p_i, q_i) for integer values of p_i and q_i. This means that L_i runs p_i times around one « arm » of the torus, and q_i times around the other. We shall make use of this remark later on.

Coming back to the pentagrid, the above labelling of the grid lines implies that any mesh of the pentagrid with no inner point belonging to the grid can be labelled by 5 indices (k_0, k_1, k_2, k_3, k_4) which are the higher indices (for each i) of the bounding lines of the polygon, and also the coordinates of the « highest » vertex of the hypercube which is cut along this polygon ; furthermore, this vertex belongs to the strip.

While the vectors $\boldsymbol{\omega}_i$ are along the directions of the five bundles of the grid, the normals $\boldsymbol{\mu}_i$ to these directions are

$$\boldsymbol{\mu}_i = \frac{(\boldsymbol{\omega}_i \cdot \mathbf{p})\,\mathbf{q} - (\boldsymbol{\omega}_i \cdot \mathbf{q})\,\mathbf{p}}{p^2 q^2 \sin^2 \varphi}, \tag{5}$$

where φ is the angle between $\mathbf{p}$ and $\mathbf{q}$. The vectors $\boldsymbol{\mu}_i$ are the projections of the standard vectors $\mathbf{e}_i$ upon the P_{pq} plane, as $\mathbf{e}_i \cdot \mathbf{p} = p_i$ and $\mathbf{e}_i \cdot \mathbf{q} = q_i$, and from (4) and (5) $\boldsymbol{\mu} \cdot \mathbf{p} = p_i$ and $\boldsymbol{\mu}_i \cdot \mathbf{q} = q_i$. Any point belonging to the set F_i obeys

$$\mathbf{OM}_i \cdot \boldsymbol{\mu}_i = k_i, \tag{6}$$

where $\mathbf{OM}_i$ is the vector to a point M_i. Hence, the periodicity of the F_i bundle is $1/|\mu_i| = pq \sin \varphi / |\boldsymbol{\omega}_i|$. In addition, using (3),

$$\sum \boldsymbol{\omega}_i = \sum \boldsymbol{\mu}_i = 0. \tag{7}$$

Thus, we can define a pentagrid on the P_{pq}-plane in a complete analogy with de Bruijn pentagrid defined on the irrational plane P.

If the origin of P_{pq} is not chosen at the origin of the axes of the 5-dimensional hyperspace, but at a point $\boldsymbol{\gamma} = (\gamma_0, \gamma_1, \gamma_2, \gamma_3, \gamma_4)$ of the first unit cell of the hypercubic lattice, we replace (6) by

$$\mathbf{OM}_i \cdot \boldsymbol{\mu}_i + \gamma_i = k_i. \tag{8}$$

The Penrose tiling is usually constructed for the case in which $\sum \gamma_i =$ integer. The extension to any value of $\gamma = \sum \gamma_i$ does not raise any difficulty, as shown by Pavlovitch and Kléman [19] in the perfect case. But approximants with an arbitrary value of γ involve mismatches which do not appear in the case $\gamma =$ integer. In the following, we shall consider only the $\gamma = 0$ approximants. In that case it is easy to show, using (7) and (8), that the sum $K = \sum k_i$ in a mesh of the pentagrid takes only 4 successive values, for example, 1, 2, 3 and 4.

3.4 Dual of the pentagrid : the tiling of a general approximant. — The dual of the pentagrid is obtained by projecting the vertices of the strip on P_{pq} ; they build a tiling whose vertices have the coordinates

$$\mathbf{R} = \sum k_i \boldsymbol{\mu}_i, \tag{9}$$

and is made of ten different shapes. It is in fact more instructive, and more natural, to project the vertices of the strip directly on the irrational plane P. One gets then two possible tilings, either

$$\mathbf{S} = \sum k_i \tilde{\boldsymbol{\mu}}_i, \tag{10}$$

where the vectors $\tilde{\boldsymbol{\mu}}_i$ are the projections of the vector $\boldsymbol{\mu}_i$ on P (such a tiling has still ten different shapes), or

$$\mathbf{T} = \sum k_i \boldsymbol{\nu}_i, \tag{11}$$

where the vectors $\boldsymbol{\nu}_i$ are directed along the sides of a regular pentagon. In the latter case, the two usual tiles of the Penrose pattern are sufficient. We present the approximant tiling in the form (11).

In fact, the pentagrid in the P_{pq}-plane can be projected onto the P-plane. This is done as follows. We project the vectors $\mathbf{p}$ and $\mathbf{q}$ (Eq. (2)) which define the P_{pq}-plane, onto the irrational plane P, defined by the vectors $\mathbf{u}_1$ and $\mathbf{u}_2$ (Eq. (1)). A straightforward calculation gives

$$\tilde{p}_j = \frac{2}{5} \sum_i p_i \cos \frac{2\pi}{5}(i - j), \quad j = 0, 1, 2, 3, 4, \tag{12}$$

where $\tilde{\mathbf{p}}$ is the projection of $\mathbf{p}$ in P-plane, and an analogous expression for $\tilde{\mathbf{q}}$, the projection of $\mathbf{q}$. It follows that the projections of the vectors $\boldsymbol{\omega}_i$ onto P are

$$\tilde{\boldsymbol{\omega}}_i = q_i \tilde{\mathbf{p}}_i - p_i \tilde{\mathbf{q}}. \tag{13}$$

We are naturally led to construct a set of vectors $\tilde{\boldsymbol{\nu}}_i$, perpendicular to the $\tilde{F}_i$-sets, i.e, to $\tilde{\boldsymbol{\omega}}_i$

$$\tilde{\boldsymbol{\nu}}_i = \frac{(\tilde{\boldsymbol{\omega}}_i \cdot \tilde{\mathbf{p}})\,\tilde{\mathbf{q}} - (\tilde{\boldsymbol{\omega}}_i \cdot \tilde{\mathbf{q}})\,\tilde{\mathbf{q}}}{\tilde{p}^2 \tilde{q}^2 \sin^2 \psi}, \tag{14}$$

where ψ is the angle between $\tilde{\mathbf{p}}$ and $\tilde{\mathbf{q}}$. But note that $\tilde{\boldsymbol{\nu}}_i$ are not the projections of the set $\boldsymbol{\mu}_i$. The period of the bundle $\tilde{F}_i$ is thus

$$\tilde{d}_i = \tilde{p}\tilde{q} \sin \psi / |\tilde{\boldsymbol{\omega}}_i| . \tag{15}$$

Let us now compare the vector products

$$\begin{aligned} \boldsymbol{\omega}_j \times \boldsymbol{\omega}_{j+1} &= (q_j p_{j+1} - p_j q_{j+1}) \, \mathbf{p} \times \mathbf{q} , \\ \tilde{\boldsymbol{\omega}}_j \times \tilde{\boldsymbol{\omega}}_{j+1} &= (q_j p_{j+1} - p_j q_{j+1}) \, \tilde{\mathbf{p}} \times \tilde{\mathbf{q}} . \end{aligned} \tag{16}$$

The two sets of vectors, $\tilde{\boldsymbol{\omega}}_i$ and $\boldsymbol{\omega}_i$, thus run around the origin in the same sense. This also holds for the two sets $\boldsymbol{\mu}_i$ and $\tilde{\boldsymbol{\nu}}_i$.

Furthermore, we can choose the p_i's and q_i's in such a way that the $\tilde{\boldsymbol{\nu}}_i$ and $\boldsymbol{\nu}_i$ rotate in the same way. If this is true, and since the sets of k_i's are the same by construction for the **R**, **S**, **T** tilings, we are sure that the topologies of these various tilings are the same. All the approximants we shall construct are such that the condition of similar rotation for the $\boldsymbol{\nu}_i$'s and $\tilde{\boldsymbol{\nu}}_i$'s is observed.

3.5 FIBONACCI APPROXIMANTS. — We now construct the rational plane P_{pq} so that it will be a Fibonacci approximant to the irrational plane P. To this end we consider the vector $\mathbf{p}$. Since it is orthogonal to the (1, 1, 1, 1, 1) direction, we can always write it in the form :

$$\mathbf{p} = \tilde{\mathbf{p}} + \tilde{\tilde{\mathbf{p}}} \tag{17}$$

where $\tilde{\mathbf{p}}$ is the projection along P (Eq. (12)) and $\tilde{\tilde{\mathbf{p}}}$ is the projection along P′, the irrational plane complementary to P. The plane P′ is defined [17] by the vectors $\mathbf{u}_3$ and $\mathbf{u}_4$

$$\begin{aligned} \mathbf{u}_3 &= \sum_j \sqrt{\frac{2}{5}} \cos \frac{4\pi j}{5} \mathbf{e}_j , \\ \mathbf{u}_4 &= \sum_j \sqrt{\frac{2}{5}} \sin \frac{4\pi j}{5} \mathbf{e}_j , \quad j = 0, 1, 2, 3, 4 . \end{aligned} \tag{18}$$

We have

$$\tilde{\tilde{\mathbf{p}}}_j = \frac{2}{5} \sum_i p_i \cos \frac{4\pi}{5} (i - j) , \quad j = 0, 1, 2, 3, 4 . \tag{19}$$

It is easily seen, from equations (12) and (19), that

$$\begin{aligned} \tilde{p}_{j+1} + \tilde{p}_{j-1} &= G\tilde{p}_j , \\ \tilde{\tilde{p}}_{j+1} + \tilde{\tilde{p}}_{j-1} &= -\tau\tilde{\tilde{p}}_j . \end{aligned} \tag{20}$$

Therefore, the vector $\tilde{\mathbf{p}}$ is given by two independent parameters alone, and so is $\tilde{\tilde{\mathbf{p}}}$. I.e.,

$$\begin{aligned} \tilde{\mathbf{p}} &= (G\tilde{p}_1 - \tilde{p}_2, \tilde{p}_1, \tilde{p}_2, G\tilde{p}_2 - \tilde{p}_1, - G\tilde{p}_1 - G\tilde{p}_2) , \\ \tilde{\tilde{\mathbf{p}}} &= (-\tau\tilde{\tilde{p}}_1 - \tilde{\tilde{p}}_2, \tilde{\tilde{p}}_1, \tilde{\tilde{p}}_2, -\tau\tilde{\tilde{p}}_2 - \tilde{\tilde{p}}_1, \tau\tilde{\tilde{p}}_1 + \tau\tilde{\tilde{p}}_2) , \end{aligned} \tag{21}$$

or any cyclic permutation of these. Written in terms of the components p_i of $\mathbf{p}$, one has

$$\begin{aligned} \tilde{\tilde{p}}_1 &= \frac{1}{\sqrt{5}} (\tau p_1 + p_3 + p_4) , \\ \tilde{\tilde{p}}_2 &= \frac{1}{\sqrt{5}} (G p_2 - p_1 - p_3) . \end{aligned} \tag{22}$$

However, the parameters $\tilde{\tilde{p}}_1$ and $\tilde{\tilde{p}}_2$ determine the distance from vertices of the reticular plane P_{pq} to the irrational P-plane. Hence, in a complete analogy with the one-dimensional case above, we choose

$$\begin{aligned} p_1 &= -(p_3 + p_4) \frac{f_m}{f_{m+1}} , \\ p_2 &= (p_1 + p_3) \frac{f_{\ell+1}}{f_\ell} , \end{aligned} \tag{23}$$

where f_ℓ and f_m are Fibonacci numbers. These choices give the best approximation to G [15] ; as in section 2, there is no vertex of the lattice between the vectors $\mathbf{p}$ or $\mathbf{q}$ and their projections on the irrational P-plane. This also yields for the vector $\mathbf{p}$ the form

$$\begin{aligned} \mathbf{p} = \frac{p_3 + p_4}{f_{m+1}} &(-f_{m-1}, -f_m, 0, f_m, f_{m-1}) + \\ &+ \frac{p_1 + p_3}{f_\ell} (-f_{\ell+1}, 0, f_{\ell+1}, f_\ell, -f_\ell) , \end{aligned} \tag{24}$$

where, of course, the linear combination can be written with any cyclic permutation of the vectors in (24). The same argumentation holds for the vector $\mathbf{q}$. We therefore may choose

$$\begin{aligned} \mathbf{p} &= (0, f_{p+1}, f_p, -f_p, -f_{p+1}) , \\ \mathbf{q} &= (-f_{q+1}, 0, f_{q+1}, f_q, -f_q) , \end{aligned} \tag{25a}$$

or

$$\begin{aligned} \mathbf{p} &= (0, f_{p+1}, f_p, -f_p, -f_{p+1}) , \\ \mathbf{q} &= (-f_q, -f_{q+1}, 0, f_{q+1}, f_q) . \end{aligned} \tag{25b}$$

The first choice corresponds to an approximant with a unit cell of the shape of a thin rhombus ; the second corresponds to an approximant with a unit cell of the shape of a thick rhombus.

These results were established for a special strip lying on a lattice plane, but extend to any rational strip. Equations (25) define the unit cell of the pentagrid and, by duality, the unit cell of the approximant. We see that along $\mathbf{p}$ the indices k_i jump by the following quantities

$$\begin{aligned} &\Delta k_0 = 0 ; \quad \Delta k_1 = f_{p+1} ; \quad \Delta k_2 = f_p ; \\ &\Delta k_3 = -f_p ; \quad \Delta k_4 = -f_{p+1} \end{aligned} \tag{26}$$

and the total index $K = \sum k_i$ does not change. In order to relate the Δk_i's to the unit cell parameter, we notice that elementary steps which do not change K consist of either a long diagonal of a thin rhombus t, or of a short diagonal of a thick rhombus T (see for example Fig. 2 of Ref. [17]). For example, a jump $\Delta k_1 = 1$ and $\Delta k_4 = -1$ is a jump along the long diagonal $\mathbf{L}_0$ of a thin rhombus perpendicular to the $\boldsymbol{\nu}_0$ direction. This is visible in figure 8, which depicts 3 lines of the pentagrid, perpendicular to $\boldsymbol{\nu}_0$, $\boldsymbol{\nu}_1$ and $\boldsymbol{\nu}_4$, respectively, such that the dual of the intersection I of 1 and 4 is a thin rhombus, whose sides are along $\boldsymbol{\nu}_1$ and $\boldsymbol{\nu}_4$. When going along the 0-direction from the mesh below I to the mesh above I, one has that $k_1 \to k_1 + 1$ and $k_4 \to k_4 - 1$. Similarly, a jump $\Delta k_2 = 1$ and $\Delta k_3 = -1$ is performed when moving along the short diagonal $\mathbf{S}_0$ of a thick rhombus, as with intersection J of 2 and 3. Thus, the lattice parameters of the approximant of equation (25a) are

$$\begin{aligned} \mathbf{b}_p &= f_{p+1}\,\mathbf{L}_0 + f_p\,\mathbf{S}_0\,, \\ \mathbf{b}_q &= f_{q+1}\,\mathbf{L}_1 + f_q\,\mathbf{S}_1\,, \end{aligned} \tag{27a}$$

while, for equation (25b) we get

$$\mathbf{b}_q = f_{q+1}\,\mathbf{L}_2 + f_q\,\mathbf{S}_2\,. \tag{27b}$$

We discuss in section 4 the implication of this relation on the properties of dislocations in approximants.

The expressions (27) of the lattice parameters do not imply that the side of the unit cell is necessarily split into S's and L's ; it is its length which is decomposable in such a way. But note that sequences of S's and L's appear along worms (Fig. 5), whose lengths $\mathbf{W}$ have been proven to have the form [18] :

$$\mathbf{W}_r = (f_r - 1)\,\mathbf{S} + (f_{r+1} - 1)\,\mathbf{L}\,.$$

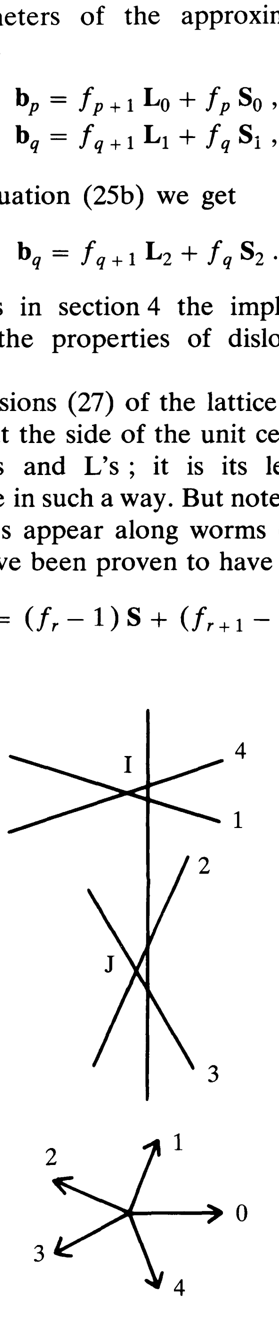

Fig. 8. — Lines of the approximant grid.

Therefore, a finite part $\mathbf{b}_p$ of a worm $\mathbf{W}_r$ (with $p < r$) can be used to construct an approximant. This observation has led us to build approximants starting from the exceptional singular Penrose tiling (all $\gamma_i = 0$), in which one has 10 semi-infinite worms originating from the central region. It appears in figure 5 that such a construction is relatively easy by hand ; the sides $\mathbf{b}_p$ and $\mathbf{b}_q$ are taken along two such semi-infinite worms and very few rearrangements are necessary to build a unit cell which tiles the plane. Other approximants of same size are obtained by propagation of mismatches (see Fig. 6).

3.6 Inflation properties and the number of mismatches of approximants. — It can be verified that going over from an approximant defined by the vectors $\mathbf{p}$ and $\mathbf{q}$ (Eq. (2)), to an approximant defined by the vectors $\mathbf{p}'$ and $\mathbf{q}'$ such that

$$p_j' = p_{j-1} + p_{j+1}\,, \quad q_j' = q_{j-1} + q_{j+1}\,, \tag{28}$$

one has

$$\boldsymbol{\omega}_i' = \boldsymbol{\omega}_{i+1} + \boldsymbol{\omega}_{i-1}\,.$$

This relation yields that in the P_{pq}-plane, the new grid is obtained from the old one by taking lines which pass through intersections of F_{i+1}-lines with F_{i-1} lines, with $k_{i+1} + k_{i-1}$ being constant. The construction is depicted in figure 9. One can show that

$$\tilde{p}' = \tau^{-1}\tilde{p}\,, \quad \tilde{q}' = \tau^{-1}\tilde{q}\,. \tag{29}$$

It follows that

$$\begin{aligned} \tilde{\boldsymbol{\omega}}_i' &= \tau^{-1}[\tilde{\boldsymbol{\omega}}_{i+1} + \tilde{\boldsymbol{\omega}}_{i-1}]\,, \\ \tilde{\boldsymbol{\nu}}_i' &= \tau^{-1}[\tilde{\nu}_{i+1} + \tilde{\nu}_{i-1}]\,. \end{aligned} \tag{30}$$

However, as opposed to the « pure » case (obtained from the irrational strip), the vector $\tilde{\boldsymbol{\omega}}_i'$ is not parallel to the vector $\tilde{\boldsymbol{\omega}}_i$, since

$$\tilde{\boldsymbol{\omega}}_{i+1} + \tilde{\boldsymbol{\omega}}_{i-1} = G\tilde{\boldsymbol{\omega}}_i - \sqrt{5}(\tilde{\tilde{q}}_i\,\tilde{\mathbf{p}} - \tilde{\tilde{p}}_i\,\tilde{\mathbf{q}})\,. \tag{31}$$

(In the pure case the last term on the r.h.s. of (31) disappears.) It means that the grid lines $\tilde{F}_i$ intersect

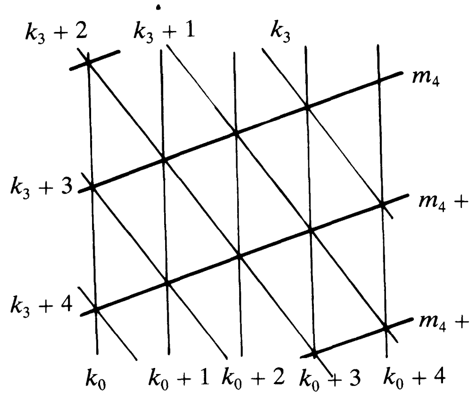

Fig. 9. — Construction of the inflated grid.

those of the grid $\tilde{F}_i'$. We shall now show that these intersections are in a one-to-one correspondence with the mismatches in the approximant tiling.

Let us first remark that there are two kinds of mismatches, which are pictured in figure 10a. They are deflated as indicated in figure 10b, where it is seen that deflation of one mismatch gives one mismatch. Therefore, the number of mismatches is invariant by inflation (or deflation). We shall retrieve this result in another way.

Consider the configuration in the pentagrid which gives a mismatch of the first type, and assume this mismatch to be perpendicular to a line of the 0-grid. The pentagrid is as in figure 11a. Note that points A and B which are duals to the thin tiles t_A and t_B are at the intersections of a 1-line and a 4-line. If, by inflation, a 0′-line passes through A and B it is the same 0′-line, because $k_1 + k_4$ takes the same value on A and B. Therefore, the 0′-line crosses the 0-line between A and B. A similar observation holds for the mismatch of the second type (Fig. 11b) which we also assume to be perpendicular to a line of the 0-grid. We consider two cases ; a) we have a succession of hexagons DQD with the mismatch between a D and a Q ; then by an argument exactly similar to above, the 0′-line AB crosses the 0-line. b) The mismatch is at the boundary between D and a decagon (Fig. 11c) and A and B are visibly on different sides of the 0-line. There are no other cases. In particular, there are never two Q hexagons in succession [18].

In summary, the number of mismatches of a grid is equal to the number of intersections of the $\tilde{F}_i$ sets with the $\tilde{F}_i'$ sets, i by i. We now derive an expression for this number.

As indicated above, we can map the unit cell of the grid of the approximant $(\mathbf{p}, \mathbf{q})$ on a 2-torus. In this mapping, each set of segments (p_i, q_i) which belong to the $\tilde{F}_i$ set, maps on a closed loop (or on

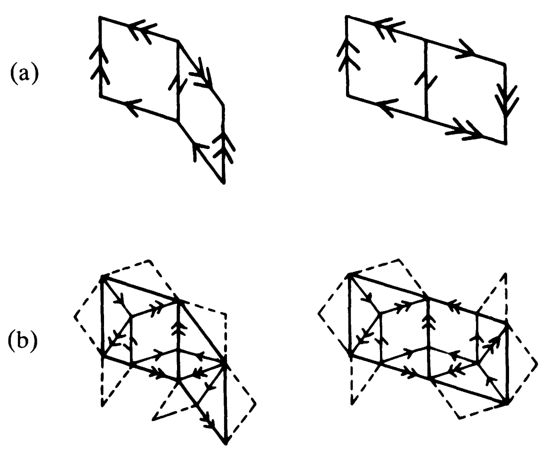

Fig. 10. — Mismatches in an undeflated and deflated tiles.

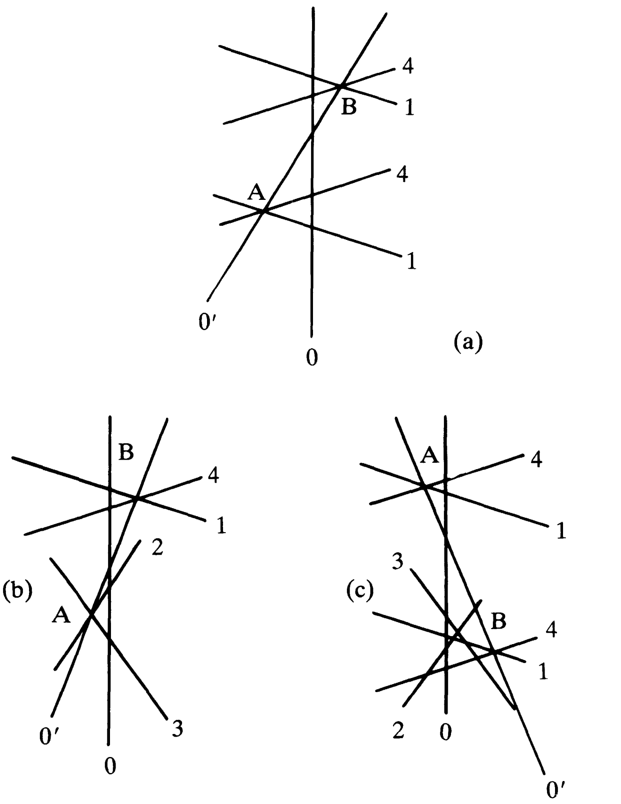

Fig. 11. — Pentagrid configurations corresponding to mismatches. a) A mismatch between two D-hexagons ; b) a mismatch between D- and Q-hexagons ; c) a mismatch between D-hexagon and a decagon.

p_i closed loops if $q_i = 0$, q_i closed loops if $p_i = 0$) of a well defined homotopy class. Now, it is easy to show that the number of intersections of the closed loop (p_i, q_i) with the closed loop (p_j, q_j) is

$$(i, j) = |p_i q_j - p_j q_i| . \tag{32}$$

The number of mismatches in the approximant $(\mathbf{p}, \mathbf{q})$ is obtained as the sum of the number of intersections of (p_i, q_i) with $(p_{i+1} + p_{i-1}, q_{i+1} + q_{i-1})$, i.e.,

$$\{\mathbf{p}, \mathbf{q}\} = \sum_i |p_i(q_{i+1} + q_{i-1}) - q_i(p_{i+1} + p_{i-1})| . \tag{33}$$

Applying this expression to the first approximant of equations (25), denoted $\{f_p, f_q\}$, we obtain

$$\{f_p, f_q\} = 2 f_{p-q+1} , \tag{34}$$

where we have assumed $p \geqslant q$. The same result holds for the approximant of equation (25b). These results were derived using well-known relations of the Fibonacci numbers [20].

Thus, from equation (34), the number of mismatches depends only upon the difference in lengths of the two sides of the approximant unit cell. The minimal number is obtained for $p = q$ or $p = q + 1$, whatever is the size of the approximant, and it is 2. In this case, there is only one shift per unit cell and the strip of the approximant can be described as a succession of irrational strip cells separated by shifts.

3.7 DENSITY OF TILES IN FIBONACCI APPROXIMANTS. — Thin tiles t appear at the intersection of lines of type 0 and 2, 1 and 3, 2 and 4, 3 and 0, 4 and 1. Thick tiles T appear at the intersection of lines of type 0 and 1, 1 and 2, 2 and 3, 3 and 4, 4 and 0. We therefore have that the numbers n_t of thin tiles and n_T of thick tiles, per unit cell, are

$$\begin{aligned} n_t &= (0,2) + (1,3) + (2,4) + (3,0) + (4,1) , \\ n_T &= (0,1) + (1,2) + (2,3) + (3,4) + (4,0) , \end{aligned} \tag{35}$$

where (i, j) is given by equation (32).

We shall now find the packing fraction

$$d = \frac{1 + n_T/n_t}{1 + \tau n_T/n_t} , \tag{36}$$

defined as the total number of tiles divided by their total area. (Note that the area of the thick rhombus is τ times the area of the thin rhombus.) For the perfect Penrose tiling, $n_T/n_t = \tau$, and $d = 0.7236...$

In order to calculate n_t and n_T we note that

$$f_p f_q = f_m^2 + (-1)^{p+1} f_n^2 , \quad p + q = 2m , \quad p - q = 2n , \tag{37}$$

for p and q of the same parity, with $p \geqslant q$. For p and q of different parity, also with $p \geqslant q$, we have :

$$f_p f_q = f_m f_{m+1} + (-1)^p f_n f_{n+1} , \quad p + q = 2m + 1 , \quad p - q = 2n + 1 . \tag{38}$$

Consequently, from equations (35), the thin approximant of (25a) has

$$\begin{aligned} n_t &= 5 f_m f_{m+1} + (-1)^m , \\ n_T &= 5 f_{m+1}^2 + 2(-1)^{m+1} , \end{aligned} \tag{39}$$

for p and q of the same parity, and

$$\begin{aligned} n_t &= 5 f_{m+1}^2 + 2(-1)^{m+1} , \\ n_T &= 5 f_{m+1} f_{m+2} + (-1)^{m+1} . \end{aligned} \tag{40}$$

for p and q of opposite parity. For the thick approximant of (25b), we find

$$\begin{aligned} n_t &= 5 f_m^2 + 2(-1)^m , \\ n_T &= 5 f_m f_{m+1} + (-1)^m , \end{aligned} \tag{41}$$

for p and q of the same parity, and

$$\begin{aligned} n_t &= 5 f_m f_{m+1} + (-1)^m , \\ n_T &= 5 f_{m+1}^2 + 2(-1)^m , \end{aligned} \tag{42}$$

for p and q of opposite parity. In any case, the number of tiles depends only upon $p + q$, i.e., upon the perimeter of the unit cell. Some representative values of the packing fraction are given in table I. We see that the perfect Penrose tiling limit is reached from below when one uses equation (39) (or Eq. (42)) and from above when equation (40) or equation (41) are used. In any case it is very close to the perfect value, and converges to it rather fast. Thus, the question of the low density of the tiles, as compared to experimental situations, cannot be resolved by the approximants.

Table I. — *The numbers of tiles per unit cell, n_t and n_T, and the packing fractions d calculated from equations* (36) *and* (39), *for the first four entries, and from* (36) *and* (40), *for the last four entries.*

m	n_t	n_T	d
1	4	7	0.7177
2	11	18	0.7228
3	29	47	0.7235
4	76	123	0.7236
1	7	11	0.7258
2	18	29	0.7239
3	47	76	0.7237
4	123	199	0.7236

4. Discussion.

We have presented a systematic study of the geometrical properties of periodic approximants for the Penrose tiling. In particular, we have constructed the rational strip which is a Fibonacci approximant of the Penrose tiling, and which yields the minimal number of shifts required to transform the perfect tiling into a periodic one. We have found a general expression for this number and shown that its minimum is 1. In addition, we have calculated the density of the tiles for the approximants, and compared it with the perfect case.

A last remark concerns our pictorial description of the geometrical properties of the approximant which is obtained by projecting on the irrational plane P. This has allowed us to carry out easy comparisons between the approximants and the Penrose tiling, because the tiles are the same. But there is of course no special reason for this projection to be the physical one ; on the contrary, the pentagonal or icosahedral symmetries should be specific of the irrational tiling, and it is known furthermore that the physical rational phases related to the quasi-crystals are often cubic, rather than rhombohedral. But since a simple affinity relates the various unit cells of various symmetry groups, we lose nothing of the topological properties of the approximants in our projection, and gain simplicity.

A special attention has been paid to the description of the approximants in terms of perfect tilings with defects. These defects are the located phason modes which have been already introduced by Socolar *et al.* [9] as basic ingredients of the field of distortion around a dislocation. Since the concept of phason mode loses its meaning in a rational structure, let us give them here another interpretation which is a generalization of the concept of discommensuration : in the cut and strip method they appear akin to intersections of the physical plane with the complementary plane (this intersection is a point), i.e., they are of the same nature as the walls which achieve the « vernier » effect in 1-d commensurate-incommensurate transition ; in a second step, these « walls » extend along the « worms » by the process described above, in the form of stacking faults.

Let us come back now to the relationship we have established between the periods of the approximants and the characteristic vectors of the Penrose tiling (Eq. (27)). Of course, the same relationship holds, topologically, if we consider an affine version of the approximant, so that we have not to worry about the exact group of symmetry of the approximant. Equation (27) tells us that the perfect dislocations of the approximant (of basic Burgers' vectors $\mathbf{b}_p$, $\mathbf{b}_q$) are split into partials of Burgers' vectors $\mathbf{L}_0$, $\mathbf{S}_0$, $\mathbf{L}_1$, $\mathbf{S}_1$, etc...

The $\mathbf{L}_i$'s and $\mathbf{S}_i$'s Burgers' vectors are small and lead to small elastic energies proportional to $|\mathbf{L}_i|^2$ and $|\mathbf{S}_i|^2$; furthermore the corresponding dislocations are akin to the dislocations of the quasi-crystals [21]. It is intriguing that such partials of the approximants, although quite similar to the elementary dislocations of the quasi-crystals, i.e., they have the same coordinates in the 5-d representation, do not carry phason distorsions *stricto sensu* (since the phason concept, as it is discussed in [9], does not belong to the realm of crystals), but they are anyway attended to by distortion akin to mismatches [22]. We point out that only partial dislocation $\mathbf{L}_i$ or $\mathbf{S}_i$ of the approximant carry mismatches. If several of them sum of a perfect dislocation of the approximant, then their mismatches can be removed altogether. Whether the large Burgers' vectors dislocations of the approximants are split or not in reality depends mostly on the energy of the mismatch field surrounding the partials ; we gather that in most cases this energy is fairly small, and that the splitting will be favoured. This should in turn play a fundamental role in the plasticity of approximants. It is well known that quasi-crystals are mechanically very hard and brittle (see [23] for a theoretical discussion) ; the simplest way to explain that fact is that, since there are no translational symmetries, there cannot be glide planes (in the metallurgical sense [24]), so that any dislocation motion is non-conservative. Related crystalline phases share most probably the same metallurgical properties of hardness and brittleness, which are well documented by the way in Frank and Kasper phases [25].

Most of the experimental work is carried out on 3-d systems. For example, Cassada *et al.* [1] have recently reported a structural transformation from a low temperature *i*-phase to a high temperature FK phase, and Rivier [26] describes grain boundaries in terms of quasi-crystals and of their approximants. Other examples of coexistence of *i*-phases and of their approximants have been given by Loiseau *et al.* [5]. The Fibonacci approximants are the periodic phases closest, structurally, to the *i*-phases. We hope that the extension of our work to the 3-d case might be useful in analyzing the appearance of structural defects in such a transformation.

However, in 3-d, the icosahedral packing of atoms is locally very compact. The cut and strip method with the unit cell as the acceptance domain yields a rather low packing fraction for the tiles. We have found in the 2-d case that by introducing stacking faults and changing the aperiodic structure into a periodic one, we can either increase or decrease the packing fraction by a small amount. A way to mimic the experimental density is to « decorate » the tiling, or to introduce additional defects [12]. Our study refers to the Bravais lattice of the 2-d pentagonal phase, and is of course not incompatible with any decoration.

Acknowledgements.

This research has been supported in part by the Fund for Basic Research administered by the Israel Academy of Sciences and Humanities and by the CNRS.

References

[1] HENLEY, C. L. and ELSER, V., *Philos. Mag.* **B 53** (1986) L 59 ;
CASSADA, W. A., SHEN, Y., POON, S. J. and SIFLET, G. J., *Phys. Rev.* **B 34** (1986) 7413.

[2] KUO, K. H., *J. Phys. France* **47** (1986) C3-425.
YUNG, Q. B. and KUO, K. H., *Philos. Mag.* **B 53**, L 115 (1986).

[3] GUYOT, P., AUDIER, M. and LEQUETTE, R., *J. Phys. France* **47** (1986) C3-405.

[4] ELSER, V. and HENLEY, C. L., *Phys. Rev. Lett.* **55** (1985) 2883 ;
HENLEY, C. L., *J. Non Cryst. Solids* **75** (1985) 91.

[5] LOISEAU, A. and LAPASSET, G., *J. Phys. France* **47** (1986) C3-331.

[6] OHASHI, W. and SPAEPEN, F., Harvard University preprint, 1987.

[7] FRANK, F. C. and KASPER, J. S., *Acta Cryst.* **11** (1958) 184 ; *Acta Cryst.* **12** (1959) 483 ;
SINHA, A. K., in *Prog. Mater. Sci.* **15** Eds. B. Chalmers, J. W. Christian and T. B. Massalski (Pergamon Press, 1972), p. 79.

[8] LUBENSKY, T. C., SOCOLAR, J. E. S., STEINHARDT, P. J., BANCEL, P. A. and HEINEY, P. A., *Phys. Rev. Lett.* **57** (1986) 1440 ;
HORN, P. M., MALZFELDT, W., DI VINCENZO, D. P., TOKERAND, J. and GAMBINO, R., *Phys. Rev. Lett.* **57** (1986) 1444.

[9] SOCOLAR, J. E. S., LUBENSKY, T. C. and STEINHARDT, P. J., *Phys. Rev.* **B 34** (1986) 3345.

[10] CHAKRABORTY, B., SOOD, A. K. and VALSAKUMAR, M. C., *Phys. Rev.* **B 34** (1986) 8202.

[11] BIHAM, O., MUKAMEL, D. and SHTRIKMAN, S., *Phys. Rev. Lett.* **56** (1986) 2191.

[12] HENLEY, C. L., *Phys. Rev.* **B 34** (1986) 797 ;
FRENKEL, D. M., HENLEY, C. L. and SIGGIA, E. D., *Phys. Rev.* **B 34** (1986) 3649.

[13] FRANK, F. C. and VAN DER MERWE, J. H., *Proc. R. Soc.* **A 189** (1949) 205 ;
FRIEDEL, J., Orsay preprint (1986).

[14] JANSSEN, T., *Acta Cryst.* **A 42** (1986) 261.

[15] NIVEN, I., *Irrational Numbers* (Wiley and Sons, Inc., New-Jersey) 1956.

[16] PEYRARD, M. and AUBRY, S., *J. Phys.* **C 16** (1983) 1593.

[17] DE BRUIJN, N. G., *K. Neder. Akad. Wetensch. Proc.* **A 84** (1981) 51.

[18] PAVLOVITCH, A., GEFEN, Y. and KLEMAN, M., in preparation.

[19] PAVLOVITCH, A. and KLEMAN, M., *J. Phys.* **A 20** (1987) 687.

[20] COXETER, H. S. M., *Introduction to Geometry* (Wiley and Sons, Inc. Toronto) 1969.

[21] KLEMAN, M., GEFEN, Y. and PAVLOVITCH, A., *Europhys. Lett.* **1** (1986) 61 ;
LEVINE, D. and STEINHARDT, P. J., *Phys. Rev. Lett.* **53** (1984) 2477 ;
LEVINE, D., LUBENSKY, T. C., OSTLUND, S., RAMASWAMY, S. and STEINHARDT, P. J., *Phys. Rev. Lett.* **54** (1985) 1520.

[22] We thank P. J. Steinhardt for pointing this interesting comment to us.

[23] LUBENSKY, T. C., RAMASWAMY, S. and TONER, J., *Phys. Rev.* **B 32** (1985) 7444.

[24] FRIEDEL, J., *Dislocations* (Pergamon Press), 1964.

[25] FRANK, F. C., private communication.

[26] RIVIER, N., *J. Phys. France* **47** (1986) C3-299 ; preprint, Imperial College (1987).